A Heat Exchanger by Using MFRD Transfer Heat from a Heat Source to a Heat Sink

Yuhua Huo

A Thesis

in

the Department

of

Mechanical and Industrial Engineering

Presented in Partial Fulfillment of the Requirements
For the Degree of Master of Applied Science at
Concordia University
Montreal, Quebec, Canada

March 2002

ABSTRACT

The dimensional and dimensionless model formulating the melting and freezing processes in the melting and freezing rotating device (MFRD) are presented. The heat transfer process between the two concentric cylinders with $D/r_o < 0.01$ may be considered as that between two parallel plates with a distance of D between them. The theoretical analysis about solidification or melting of a slab at a constant boundary temperature, which is greater or lower than the melting point, is conducted. The theoretical and numerical analysis of the Quasi-Steady state with the moving phase boundaries of the melting and freezing processes in the dimensionless system are performed. Moreover, the properties in MFRD are analyzed. The use of MFRD in the aerospace is discussed.

ACKNOWLEDGEMENTS

The Master thesis "A Heat Exchanger by Using MFRD Transfer Heat from a Heat Source to a Heat Sink" is supervised by Dr. Sui Lin and co-supervised by Dr. Georgios H.Vatistas and is completed by Yuhua Huo.

I would first like to express my sincere gratitude to my supervisor Prof. Lin Sui for his advice, constant guidance and support throughout my graduate studies and for providing the opportunity, the environment and the resources to carry out this research. Without his supervision and support, I couldn't finish this thesis. I also would like to sincerely thank my supervisor Prof. Georgios H.Vatistas for his guidance and his help.

Many thanks to Dr. Tzu-Fang Chen in the Dept. of Mechanical & Industrial Engineering for his technical discussion concerns my thesis.

TABLE OF CONTENT

CHAPTER 1

Introduction of MFRD

CHAPTER 2

The Mathematical Analysis of Melting-Freezing Rotating Device

CHAPTER 3

The Analysis of Properties in MFRD

CHAPTER 4

Discussion

CHAPTER 5

Summary

CHAPTER 6

Future Work

LIST OF FIGURES

NOMENCLATURES

MFRD	Melting – freezing rotating device
PCM	The phase change material
erf( )	Error function
L	The latent heat of solidification (J/Kg)
c	The specific heat of the PCM (J/Kg K)
α	Rotating angle of MFRD
θ	Region of the melting process
n	Angular velocity n of melting-freezing rotating device (MFRD) (rps / sec)
r_i	The radii of inner cylinder (m)
r_0	The radii of outer cylinder (m)
r	Cylindrical coordinate (m)
x	orthogonal coordinate for plate case (m)
t	Time (s)
Th	The temperatures of heat source of MFRD (°C)
Tc	The temperatures of heat sink of MFRD (°C)
Ts	The temperature of solidification of phase change material (°C)
R(t)	Position of the phase front (m)

S(t)	Position of phase front in plate case (m)
D	The distance between two parallel plates (m)
S_T	Stefan number defined by equation
L_m	The effective latent heats for the melting process (J/Kg)
c_m	The specific heat of the PCM in melting phase (J/Kg K)
a_m	Thermal diffusivity of melting phase $a_m = \frac{K_m}{\rho_m C_m}$ (m^2/s)
K_m	Thermal conductivity of PCM in melting phase (W/K·m)
T_m	The temperature of PCM in melting phase (K)
ρ_m	The density of PCM in melting phase (Kg/m^3)
S_{Tm}	Stefan number for the melting process defined by equation
$R_m(t)$	Position of melting front (m)
P_m	Dimensionless constant defined by equation (2.36)
L_f	The effective latent heats for the freezing process (J/Kg)
c_f	The specific heat of the PCM in freezing phase (J/Kg K)
a_f	Thermal diffusivity of freezing phase $a_f = \frac{K_f}{\rho_f C_f}$ (m^2/s)
K_f	Thermal conductivity of PCM in freezing phase (W/K·m)
T_f	The temperature of PCM in freezing phase (K)
ρ_f	The density of PCM in freezing phase (Kg/m^3)
S_{Tf}	Stefan number for the melting process defined by equation
$R_f(t)$	Position of freezing front (m)

P_f	Dimensionless constant defined by equation (2.41)
W	The dimensionless heat transfer per unit time per unit length in longitudinal direction
Q	The heat transfer per unit length in the longitudinal direction (J/m)

CHAPTER 1

Introduction of the melting and freezing rotating device (MFRD)

1.1 Literature Survey

Condensation of vapors and the evaporation and boiling of liquids are commonplace in power and process engineering. Condensation processes require that the enthalpy of phase change be removed to a coolant, and evaporation and boiling processes require that this enthalpy be supplied from an energy source. Since the enthalpy of phase change is relatively large, the associated heat transfer rates are also usually large. In most industrial processes, the vapor and liquid phases both flow through a heat exchanger [1]. Thus, the heat transfer to the phase interface is essentially a convective process, but it is often complicated by an irregular interface, for example, bubbles or drops [2].

Melting of solids and freezing of liquids are not used in industrial heat transfer processes, because the solid phase cannot flow through a heat exchanger. However, thermal energy storage systems use liquid-solid phase change for its ease of implementation. For example, a phase-change material (PCM) can be incorporated into

the walls of an outdoor telecommunication enclosure. The PCM absorbs excess thermal energy during the peak solar heating period, by changing the solid phase to the liquid phase, and discharges the excess heat at the other time. The alternating absorbing and discharging of heat is the characteristic of the thermal energy storage system.

Recent research works in the phase change energy storage systems were conducted, for example, they are listed in References [3] to [20]. It appears that no research work is available in the literature for a heat exchanger utilizing melting and freezing of a PCM to transfer heat continuously from a heat source to a heat sink.

1.2 Introduction of Solid-Liquid Phase-Change Heat Transfer

Solid-Liquid Phase-Change (melting or solidification) heat transfer phenomena are accompanied by a phase transformation of the medium and by either absorption or release of thermal energy in the active zone. The energy absorbed or released from the surrounding system is commonly transferred by conduction or convection. The essential and common features of systems undergoing solid-liquid phase-change heat transfer are that an interface exists separating two regions of differing thermophysical properties and that a moving surface exists which separates the two phases and at which energy is absorbed or liberated.

One of the largest applications for phase-change materials (PCMs) is in passive

solar building, requiring a material melting at or just above room temperature. It also is used in metal casting, welding, coating [21].

1.3 Introduction of MFRD

1.3.1 The reasons to develop the MFRD

In aerospace, some design problems still exist by using normal thermal design method. These problems are:

1) Small satellites don't have enough areas in the outer panels to release the extra heat because of the decline of solar absorptivity at the end of life of the satellites (EOL).

2) Normal thermal design methods are difficult to deal with the instruments with irregular, instant and large heat generations.

3) It is not flexible to handle the changeable heat generations.

MFRD is developed to solve these problems easily.

Also by using normal thermal design methods in aerospace, it is very complicated. For example, we have to know the view factor of direct solar heating, albedo and planet radiations. We have to know the precise heat generations and thermal properties for every instrument. We have to finish thermal calculation according to the precise conditions. It is time consuming. However, MFRD can simplify the thermal design. The most important part for MFRD application is choosing the suitable PCM material according to the

precise conditions.

1.3.2 Introduction of MFRD

Recently, Dr.Lin and Dr. Chen developed a physical model describing the melting and freezing processes taking place in the melting and freezing rotating device (MFRD) [1]. The present study is based on the model presented in [1].

The principle of MFRD is based on the Solid-Liquid Phase-Change Heat Transfer.

Heat transfer using melting and freezing of a phase change material is usually applied to stationary energy storage systems. For example, PCMs may be incorporated in the building envelope to achieve latent heat storage. The PCM absorbs excess thermal energy during the peak solar heating period, by changing the solid phase to the liquid phase, and discharges the excess heat at the other time. However, it appears that no research work is available in the literature for a heat exchanger utilizing melting and freezing of a PCM to transfer heat continuously from a heat source to a heat sink. The PCMs have been little used in the space technology, specifically, in the thermal control subsystem of satellites.

In order to utilize melting and freezing of a PCM to transfer heat continuously from a heat source to a heat sink, a Melting-Freezing Rotating Device (MFRD) is proposed. The device consists of two concentric cylinders with a PCM filled between them. It rotates between the heat source and the heat sink. The PCM absorbs heat from the heat source, by changing the solid phase to the liquid phase, and discharges the heat to the heat sink, by

changing the liquid phase to the solid phase. The cyclic melting and freezing processes transfer heat continuously from the heat source to the heat sink. Thus, the MFRD can be used in the spinning satellites to keep the temperature of modules in the limited variation.

The advantage of the MFRD is that the PCM in the device has a large latent heat of solidification, which allows for a small size of the device with a high heat transfer capacity. It will be shown later that the device possesses a good capability of maintaining the design condition by regulating the rotating speed of the device when the amount of heat to be transferred from the heat source varies.

From the literature survey, we can see that the MFRD is the first device utilizing melting and freezing of a PCM to transfer heat continuously from a heat source to a heat sink.

Figure 1.1 shows a schematic diagram of the MFRD. During the rotation of the device, the outer cylinder is in contacts with the heat source with a rotating angle of α between 0 and θ, ($0<\alpha<\theta$). Further assumptions are made that the surface temperature of the outer cylinder in this region is equal to the temperature of the heat source, Th, which is higher than the solidification temperature of the phase change material, Ts. Therefore, a melting process takes place in the region of $0<\alpha<\theta$. The outer cylinder is also in contacts with a coolant in the region of $\theta<\alpha<2\pi$, and its surface temperature is equal to the coolant temperature, Tc, which is lower than Ts. As a result, the freezing process takes place in the region of $\theta<\alpha<2\pi$.

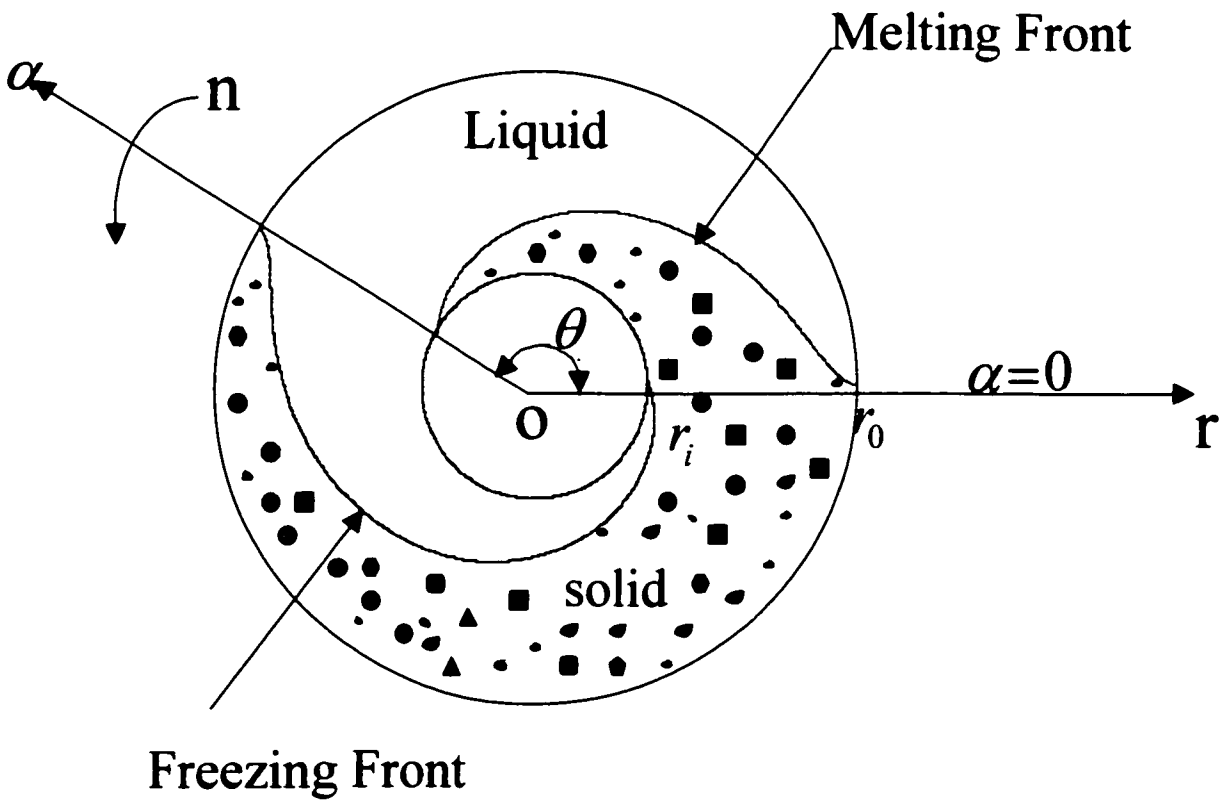

Fig 1.1 Schematic diagram of a melting-freezing rotating device

CHAPTER 2

The Mathematical Analysis of Melting-Freezing Rotating Device

2.1 Mathematical Formulation of the Melting-Freezing Rotating Device

The MFRD used to transfer heat from a heat source to a heat sink consists of two concentric cylinders with a PCM filled between them. Figure 1.1 shows a schematic diagram of the MFRD. The inner and outer cylinders have radii of r_i and r_0, respectively. The device rotates with a rotating speed of n rps. The cylinder walls are considered to be very thin and their thermal conductivities are very large, therefore, for thermal analysis, the wall thickness may be neglected.

In order to simplify the analysis, the concept of the effective latent heats, L_m and L_f, for the melting and freezing processes, respectively, is introduced. The effective latent heat includes the latent heat and the sensible heat below or above the solidification temperature of the phase change material for the melting or freezing process, respectively, as follows:

$$L_m = L + c_f (T_s - T_c) / 2 \tag{2.1}$$

$$L_f = L + c_m (T_h - T_s) / 2 \tag{2.2}$$

Where L is the latent heat of solidification and c is the specific heat of the phase change material. The subscripts, m and f, refer to the melting and freezing processes, respectively.

The introduction of the effective latent heats, L_m and L_f, simplifies the temperature distribution at the beginning of the melting or freezing process with a constant solidification temperature, Ts. Further assumption is made that, during the melting or freezing process, the thermal properties of the phase change material, in each phase, are constant, that advection is absent (i.e., the liquid is quiescent) and there is no density change across the phase boundary.

2.2 Dimensional Mathematical Equations Describing the Melting \Freezing Process

The formulation of the melting and freezing processes starts with a time transformation,

$$t = \alpha / (2\pi n) \tag{2.3}$$

For example, if $\theta = \pi$, then the times required for the complete melting and freezing processes per rotation of the device are:

$$t_{mi} = \frac{\theta}{2\pi n} = \frac{1}{2n} \tag{2.4}$$

and

$$t_{fi} = \frac{2\pi - \theta}{2\pi n} = \frac{1}{2n} \tag{2.5}$$

The governing equation describing the melting/freezing process between the two cylinders is:

$$\frac{1}{a}\frac{\partial T\,(r,t)}{\partial t} = \frac{\partial^2 T}{\partial r^2} + \frac{1}{r}\frac{\partial T}{\partial r} \tag{2.6a}$$

For the melting process, it can be written:

$$\frac{\partial T_m(r,t)}{\partial t} = \frac{a_m}{r}\frac{\partial}{\partial r}[r\frac{\partial T_m(r,t)}{\partial r}] \qquad R_m(t) < r < r_0\,, \tag{2.6b}$$

Where the subscript m refers to the melting process, a_m is the thermal diffusivity of the melting phase, and $R_m(t)$ is the location of the phase front. The boundary conditions and the energy balance at the phase front $R_m(t)$ can be expressed as:

$$T_m(r_o,t) = T_h \tag{2.7}$$

$$T_m(R_m(t),t) = T_s \tag{2.8}$$

and

$$-k_m \frac{\partial T_m(R_m(t),t)}{\partial r} = \rho L_m (\frac{dR_m(t)}{dt}) \tag{2.9}$$

Where k_m is the thermal conductivity of the melting phase and ρ is the density. The initial conditions for the temperature and the location of the phase boundary can be written as:

$$T_m(r, 0) = T_s \tag{2.10}$$

and

$$R_m(t=0)=r_o \tag{2.11}$$

The freezing process starts from the angle of θ and ends at the angle of 2π, as shown in Figure 1.1. The system of equations describes the freezing process similar to that of the melting process presented through equations (2.6b) to (2.11) as follows:

$$\frac{1}{a_f}\frac{\partial T_f(r,t)}{\partial t} = \frac{\partial T_f^{\,2}}{\partial r^2} + \frac{1}{r}\frac{\partial T_f}{\partial r}$$

$$\frac{\partial T_f(r,t)}{\partial t} = \frac{a_f}{r}\frac{\partial}{\partial r}(r\frac{\partial T_f(r,t)}{\partial t}) \quad R_f(t) < r < r_0 \tag{2.12}$$

and

$$T_f(r_0,t) = T_c \tag{2.13}$$

$$T_f(R_f(t),t) = T_s \tag{2.14}$$

$$k_f \frac{\partial T_f(R_f(t),t)}{\partial r} = \rho_f L_f(\frac{dR_f(t)}{dt}) \tag{2.15}$$

$$T_f(r,t=0) = T_s \tag{2.16}$$

$$R_f(t=0) = r_0 \tag{2.17}$$

However, no exact analytical solutions exist for the equations (2.6b) – (2.11) or (2.12) – (2.17).

2.3 Solution for the Case of Very Small Value D/r_o

If the space between the two cylinders, $D = r_o - r_i$, is very small in comparison with the radius r_o, the melting and freezing processes taking place between the two concentric cylinders of the MFRD can be presented as those taking place between the two plates. This

problem becomes the issue of solidification or melting of a slab at a constant boundary temperature, which is greater or lower than the melting point. It simplifies the thermal model and the theoretical solution can be obtained.

In this section, the effect of the very small geometrical ratio D/r_o on the heat conduction equation in the orthogonal coordinate is considered. For the purpose of simplicity, it is assumed that the boundary condition at the inner cylinder wall is insulated.

For the purpose of comparing the magnitudes of the two terms on the right-hand side of equation (2.6a), the method of scale analysis [22] is used. The first term represents the curvature of the temperature distribution in the r direction. The curvature represents the change in the slope,

$$\frac{\partial^2 T}{\partial r^2} \sim \frac{(\frac{\partial T}{\partial r})_{r=r_0} - (\frac{\partial T}{\partial r})_{r=r_i}}{r_0 - r_i} \tag{2.18}$$

in which the sign ~ means "is of the same order of magnitude as". With

$$(\frac{\partial T}{\partial r})_{r=r_0} \sim \frac{\Delta T}{r_0 - r_i}, \tag{2.19}$$

$$(\frac{\partial T}{\partial r})_{r=r_i} = 0 \qquad\qquad r_0 - r_i = D \tag{2.20}$$

the curvature becomes:

$$\frac{\partial^2 T}{\partial r^2} \sim \frac{\Delta T}{D^2} \tag{2.21}$$

The second term can be expressed as:

$$\frac{1}{r}\frac{\partial T}{\partial r} \sim \frac{1}{r_0}\frac{\Delta T}{D} \tag{2.22}$$

The ratio of equation (2.22) to equation (2.21) yields

$$\frac{\frac{1}{r}\frac{\partial T}{\partial r}}{\frac{\partial^2 T}{\partial r^2}} \sim \frac{D}{r_0} \tag{2.23}$$

A very small value of D/r_o, for example, $D/r_o < 0.01$, means that the second term is negligible small in comparison with the first term. Equation (2.6a) then becomes:

$$\frac{1}{a}\frac{\partial T\,(r,t)}{\partial t} = \frac{\partial^2 T}{\partial r^2} \tag{2.24}$$

It can be seen that the heat transfer process between the two concentric cylinders with $D/r_o < 0.01$ may be considered as that between two parallel plates with a distance of D between them.

The previous equations can be easily transformed into the orthogonal coordinate. Figure 2.1 shows a schematic diagram of a melting process between the two corresponding parallel plates. S(t) represents the locations of the phrase boundary at which the temperature is equal to the solidification temperature Ts.

A space coordinate transformation is as follows:

$$x = r_0 - r \tag{2.25}$$

$$x = 0 \qquad \text{at} \quad r = r_0 \tag{2.26}$$

$$x = D \qquad \text{at} \quad r = r_i \tag{2.27}$$

$$x = S(t) \qquad \text{at} \quad r = R(t) \tag{2.28}$$

S(t) is the location of the phase front corresponding to R(t).

The problem now is that in which the region x >0 is initially solid at temperature T_s, and for which t >0 the plane x = 0 is maintained at constant temperature $T_h > T_s$.

For the melting phrase, the equation (2.24) can be written as:

$$\frac{1}{a_m}\frac{\partial T_m(x,t)}{\partial t} = \frac{\partial^2 T_m(x,t)}{\partial x^2} \qquad 0 < x < S(t) \tag{2.29}$$

The boundary conditions and the energy balance at the phase front can be expressed as:

$$T_m(0,t) = T_h \tag{2.30}$$

$$T_m(S(t),t) = Ts \tag{2.31}$$

$$-k_m \frac{\partial T_m(S(t),t)}{\partial x} = \rho L_m \left(\frac{dS(t)}{dt}\right) \tag{2.32}$$

The initial conditions for the temperature and location of the phase boundary can be written as:

$$T_m(x,0) = T_i \tag{2.33}$$

$$S(t=0) = 0 \tag{2.34}$$

The exact solution of the above system of equations (2.29) to (2.34) is the well known Nenmann's solution [23] which can be expressed as:

$$T_m(x,t) = T_h - \frac{(T_h - T_s)}{erf(P_m)} erf(\frac{x}{\sqrt{4a_m t}}) \tag{2.35}$$

Where erf( ) is the error function and p_m is a numerical constant defined by

$$S_m(t) = P_m \sqrt{4a_m t} \tag{2.36}$$

The constant of p_m is determined from equation (2.32) as follows:

$$\sqrt{\pi} P_m \exp(P_m^2) erf(P_m) = S_{Tm} \tag{2.37}$$

Where S_{Tm} is the Stefan number for the melting process defined by:

$$S_{Tm} = \frac{C_m}{L_m}(T_h - T_s) \tag{2.38}$$

The maximum location of the moving phase front is the space D between the two concentric cylinders. The time required for Rm(tmD) = r_i in the melting process is given from equation (2.36) as follows:

$$t_{mD} = \frac{D^2}{4a_m P_m^2} \tag{2.39}$$

The freezing process starts from the angle of θ and ends at the angle of 2π, as shown in Figure 1.1. The system of equations describes the freezing process is the same as that describes the melting process, except that no minus sign in equation (2.32), that the subscript m is replaced by f referring to the solid phase in the freezing process, and that the heat source temperature, T_h, in equation (2.30) is changed to the coolant temperature, T_c. The exact Neumann's solution for the freezing process is:

$$T_f(x,t) = T_c + \frac{(T_s - T_c)}{erf(P_f)} erf(\frac{x}{\sqrt{4a_f t}}) \tag{2.40}$$

P_f is a dimensionless constant defined by

$$S_f(t) = P_f \sqrt{4a_f t} \tag{2.41}$$

The value of P_f is determined from equation (2.32) with the change of the subscript m to s and without the minus sign.

$$\sqrt{\pi} P_f \exp(P_f^2) erf(P_f) = S_{Tf} \tag{2.42}$$

Where S_{Tf} is the Stefan number for the freezing process defined by:

$$S_{Tf} = \frac{C_f}{L_f}(T_s - T_c) \tag{2.43}$$

The maximum location of the moving phase front is the space between the two concentric cylinders, D. The time required for $S(t_{fD}) = D$ in the freezing process is given from equation (2.41).

$$t_{fD} = \frac{D^2}{4a_f P_f^2} \tag{2.44}$$

Obviously, equation (2.37) and (2.42) are identical, except the subscripts. So the two equations can be plotted together in one diagram as shown in Figure 2.2.

2.4 Determination of Design Parameters

The design parameters involve in the MFRD are the rotating speed of the device, n, the radius of the outer cylinder, r_o, the space between the two concentric cylinders, D, and the contact angle between the outer cylinder and the heat source during the melting process, θ. These parameters need to be determined from the analysis.

The design parameters, θ, D, n, and r_o, are determined as follows:

Step 1. Determination of p_m and p_f:

Calculate the Stefan numbers, S_{Tm} and S_{Tf}, from equations (2.38) and (2.43), respectively, and determine the dimensionless constants, p_f and p_m, from Figure 2.2.

Step 2. Determination of θ:

Eliminating D from equations (2.39) and (2.44) gives:

$$\frac{t_{mD}}{t_{fD}} = \frac{a_f P_f^2}{a_m P_m^2} \tag{2.45}$$

From geometrical point of view, as shown in Figure 1.1, the time ratio presented in equation (2.45) can also be expressed as:

$$\frac{t_{mD}}{t_{fD}} = \frac{\theta}{2\pi - \theta} \tag{2.46}$$

Eliminating the time ratio from equations (2.45) and (2.46), the angle, θ , representing the region of the melting process, is obtained as:

$$\theta = \frac{2\pi}{1 + \frac{a_m}{a_f}(\frac{P_m}{P_f})^2} \tag{2.47}$$

Step 3. Determination of $D^2 n$

The rotating time of the device for the melting process can be calculated by:

$$t_{mD} = \frac{\theta}{2\pi n} \tag{2.48}$$

Elimination of the time, t_{mD}, from equations (2.39) and (2.48), gives the combination of the two design parameters, D and n,

$$D^2 n = \frac{2a_m P_m^2 \theta}{\pi} \tag{2.49}$$

Step 4. Determination of D/r_o:

The radius of the outer cylinder, r_o, is determined from the amount of the heat to be transferred from the heat source to heat sink as follows,

$$r_0 = \frac{q}{\rho L_m \theta D n} \tag{2.50}$$

Eliminating the rotating speed of the device, n, from equations (2.49) and (2.50), yields the geometric ratio of the device,

$$\frac{D}{r_0} = 2a_m P_m^2 \rho L_m \theta^2 / (\pi q) \tag{2.51}$$

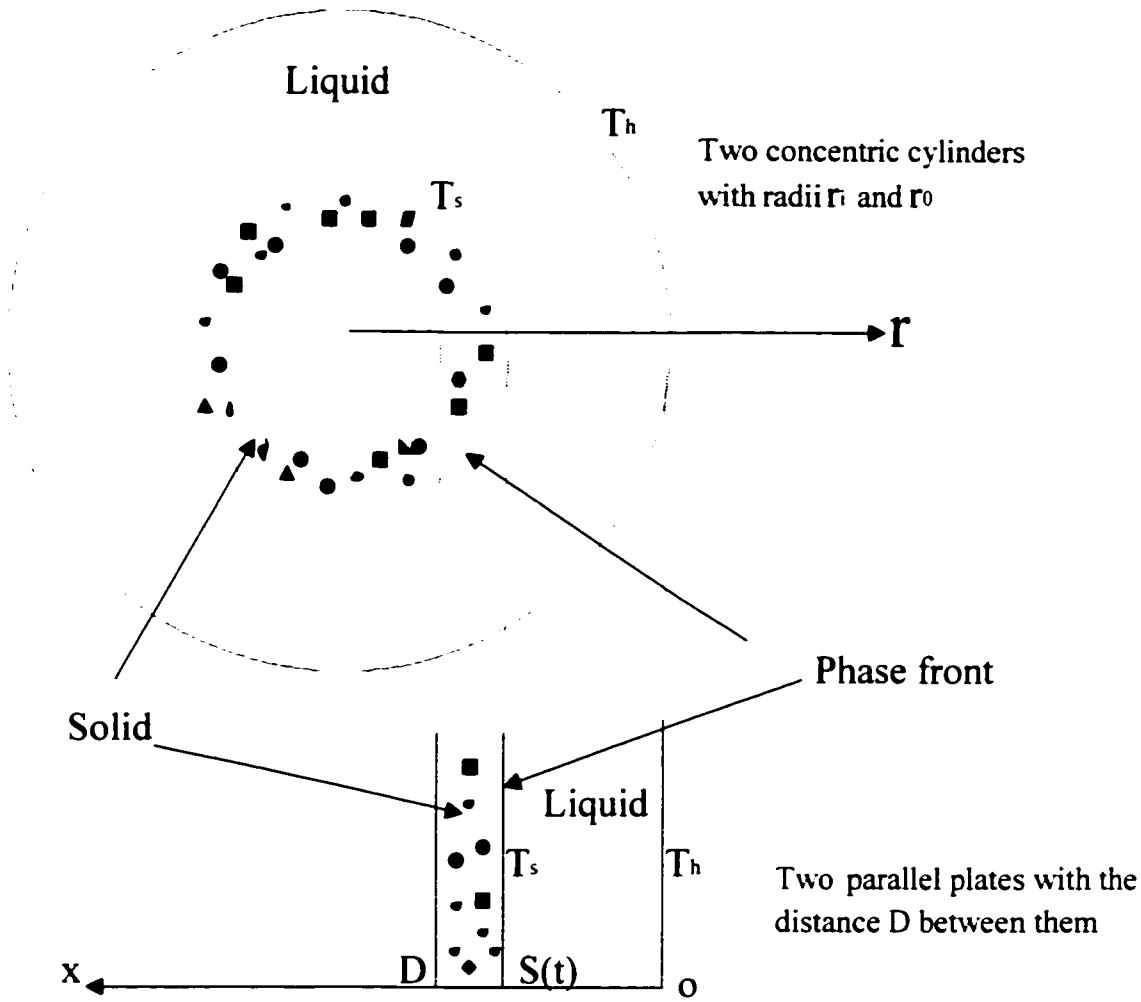

Figure 2.1 Schematic diagram of a melting process between two concentric cylinders without rotation and between two corresponding parallel plates. R(t) and S(t) represent the locations of the phase boundary.

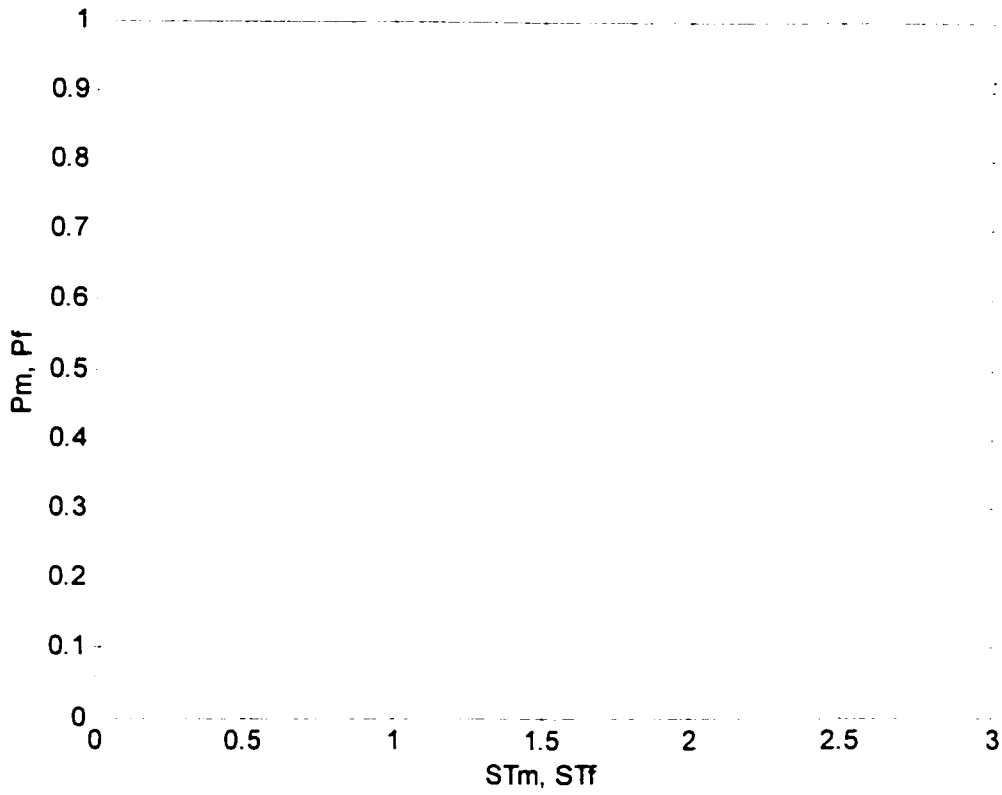

Fig 2.2 Dimensionless constants Pm and Pf as the function of Stefan number [1]

2.5 Dimensionless Mathematical Equations Describing the Melting \ Freezing Process

The equations formulating the melting and freezing processes in the MFRD are also transformed to a dimensionless form. In this section, the dimensionless parameters governing the phase-change heat transfer are presented. The dimensionless parameters, which delineate the heat transfer regimes, evolve from the transformation of the basic equations to a dimensionless form.

In the dimensionless form, variables are organized into groups, which can be considered as new variables. These new variables will be fewer in number because of their grouping. Therefore, fewer data are needed to determine relationships, and the problem of data presentation is simplified. This is the advantage of the dimensionless analysis. In order to obtain an analytical solution of the dimensionless equations, the quasi-steady approximation is utilized.

For the purpose of simplifying the analysis, the following dimensionless parameters are introduced:

$$T_m^* = \frac{T_m - T_s}{T_h - T_s} \tag{2.52}$$

$$T_f^* = \frac{T_f - T_s}{T_c - T_s} \tag{2.53}$$

$$t^* = \frac{a_m t}{r_0^2} \tag{2.54}$$

$$n^* = \frac{n r_0^2}{a_m} \tag{2.55}$$

$$r^* = \frac{r}{r_0} \tag{2.56}$$

$$r_i^* = \frac{r_i}{r_0} \tag{2.57}$$

and

$$r_o^* = 1 \tag{2.58}$$

$$R_m^*(t^*) = \frac{R_m(t)}{r_0} \tag{2.59}$$

$$R_f^*(t^*) = \frac{R_f(t)}{r_0} \tag{2.60}$$

$$S_{Tm} = \frac{C_m}{L_m}(T_h - T_s) \tag{2.61}$$

$$S_{Tf}^{\bullet} = \frac{a_f}{a_m}\frac{C_f}{L_f}(T_s - T_c) \tag{2.62}$$

Where S_{Tm} and $S_{Tf}^{\bullet}$ are the Stefan number. With the relations of equations (2.54) and (2.55), equations (2.3) to (2.5) can be written as:

$$t^{\bullet} = \frac{\alpha}{2\pi n^{\bullet}} \tag{2.63a}$$

and if $\theta = \pi$:

$$t_i^{\bullet} = t_{mi}^{\bullet} = t_{fi}^{\bullet} = \frac{1}{2n^{\bullet}} \tag{2.63b}$$

With the above dimensionless parameters, equations (2.6b) to (2.11) for the melting process and equations (2.12) to (2.17) for the freezing process become dimensionless as follows:

The melting process:

$$\frac{\partial T_m^{\bullet}}{\partial t^{\bullet}} = \frac{1}{r^{\bullet}}\frac{\partial}{\partial r^{\bullet}}(r^{\bullet}\frac{\partial T_m^{\bullet}}{\partial r^{\bullet}}) \tag{2.64}$$

$$T_m^{\bullet}(1, t^{\bullet}) = 1 \tag{2.65}$$

$$T_m^*(R_m^*(t^*),t^*) = 0 \tag{2.66}$$

and

$$-S_{Tm}\frac{\partial T_m^*(R_m^*(t^*),t^*)}{\partial r^*} = \frac{dR^*_m(t^*)}{dt^*} \tag{2.67}$$

$$T_m^*(r^*,t^* = 0) = 0 \tag{2.68}$$

$$R_m^*(t^* = 0) = 1 \tag{2.69}$$

The freezing process:

$$\frac{\partial T_f^*}{\partial t^*} = \frac{a_f}{a_m}\frac{1}{r^*}\frac{\partial}{\partial r^*}(r^*\frac{\partial T_f^*}{\partial r^*}) \tag{2.70}$$

and

$$T_f^*(1,t^*) = 0 \tag{2.71}$$

$$T_f^*(R_f^*(t^*),t^*) = 1 \tag{2.72}$$

$$S_{Tf}\frac{\partial T_f^*(R_f^*(t^*),t^*)}{\partial r^*} = \frac{dR_f(t^*)}{dt^*} \tag{2.73}$$

$$T_f^*(r^*, t^* = 0) = 1 \tag{2.74}$$

$$R_f^*(t^* = 0) = 1 \tag{2.75}$$

Since the phase front moves relatively slowly, an assumption can be made that the moving phase front does not have a major inference on the temperature distribution during a short period of time. Thus, the quasi-steady approximation may be applied for equations (2.64) and (2.70) to yield:

for the melting process:

$$\frac{\partial}{\partial r^*}(r^* \frac{\partial T_m^*(r^*, t^*)}{\partial r^*}) = 0 \tag{2.76}$$

and for the freezing process:

$$\frac{\partial}{\partial r^*}(r^* \frac{\partial T_f^*(r^*, t^*)}{\partial r^*}) = 0 \tag{2.77}$$

The solution of equation (2.76) with the boundary conditions, equations (2.65) and (2.66), is:

$$T_m^* = 1 - \frac{\ln r^*}{\ln R_m^*} \tag{2.78}$$

Substitution of equation (2.78) into equation (2.67) gives:

$$\frac{dR_m^*}{dt^*} = \frac{S_{tm}}{R_m^* \ln R_m^*} \tag{2.79}$$

Integration of equation (2.79) with initial condition, equation (2.69), yields:

$$R_m^{*2} \ln R_m^* - \frac{1}{2}(R_m^{*2} - 1) = 2S_{Tm} t^* \tag{2.80}$$

At the end of the melting process, $R_m^* = r_i^*$, the time required is equal to t_i^*. Equation (2.80) becomes:

$$r_i^{*2} \ln r_i^* - \frac{1}{2}(r_i^{*2} - 1) = 2S_{Tm} t_i^* \tag{2.81}$$

The solution of equation (2.77) with the boundary conditions, equations (2.71) and (2.72), is:

$$T_f^* = \frac{\ln(r^*)}{\ln(R_f^*)} \tag{2.82}$$

Substitution equation (2.82) into equation (2.73) gives:

$$\frac{dR_f^*}{dt^*} = \frac{S_{Tf}}{R_f^* \ln R_f^*} \tag{2.83}$$

Integration of equation (2.83) with initial condition, equation (2.75) yields:

$$R_f^{*2} \ln R_f^* - \frac{1}{2}(R_f^{*2} - 1) = 2S_{Tf} t^* \tag{2.84}$$

At the end of the freezing process, $R_f^* = r_i^*$, the time required is equal to be t_i^*. Equation (2.84) becomes:

$$r_i^{*2} \ln r_i^* - \frac{1}{2}(r_i^{*2} - 1) = 2S_{Tf} t_i^* \tag{2.85}$$

If $\theta = \pi$, comparison of equation (2.81) with equation (2.85) indicates:

$$S_{Tm} = S_{Tf} \tag{2.86}$$

Comparing the equation (2.80) and equation (2.84) gives:

$$R_m^* = R_f^* \tag{2.87}$$

It can be seen that equations (2.80) to (2.81) are identical to equations (2.84) to (2.85). This means that the moving phase boundaries of the melting and freezing process taking place in the MFRD are identical to each other. The only exception is that the melting process starts at $\alpha = 0$ and ends at $\alpha = \pi$, and that the freezing process starts at $\alpha = \pi$ and ends at $\alpha = 2\pi$. Therefore, the subscripts m and f are omitted in the equations of the following discussion.

CHAPTER 3

The Analysis of Properties in MFRD

3.1 The Analysis of Dimensionless Heat Transfer W

3.1.1 The Definition of Dimensionless Heat Transfer W

In this section, the contact angle of heat source or heat sink $\theta = \pi$ and the unit length in the longitudinal direction are assumed.

The heat transfer per unit length in the longitudinal direction is:

$$Q = \frac{\pi}{2}(r_0^2 - r_i^2) \times 1 \times \rho L \tag{3.1}$$

The expression $(\frac{\pi}{2}(r_0^2 - r_i^2) \times 1)$ means the volume of the PCM melting or freezing phrase.

The time required for $R = r_i$ in melting/freezing process as shown in the equations (2.81) or (2.85).

$$r_i^{*2} \ln r_i^* - \frac{1}{2}(r_i^{*2} - 1) = 2S_T t_i^*$$

For the melting process, it can be written as follows:

$$r_i^{*2} \ln r_i^* - \frac{1}{2}(r_i^{*2} - 1) = 2S_{Tm} \frac{a_m t_i}{r_0^2} \tag{3.2}$$

It can also be written for the melting process as follows:

$$t_i = \frac{r_i^{*2} \ln r_i^* - \frac{1}{2}(r_i^{*2} - 1)}{2a_m \times \frac{c_m}{L_m}(T_h - T_s)} \times r_0^2 \tag{3.3}$$

Define the dimensionless heat transfer per unit time per unit length in the longitudinal direction as W.

$$W = \frac{Q}{t \times k_m \times (T_h - T_s)} \tag{3.4}$$

By using equation (3.1) and (3.3), equation (3.4) becomes:

$$W = \frac{\pi(1 - r_i^{*2})}{r_i^{*2} \times \ln r_i^{*} + \frac{1}{2}(1 - r_i^{*2})} \tag{3.5}$$

Figure 3.1a and Figure 3.1b illustrate the relationship between W and r_i^{*}.

3.1.2 The Analysis of the results

Figure 3.1a and Figure 3.1b illustrate some proprieties.

1) The W of MFRD is constant while r_i is infinitesimal

When $r_i^{*} \to 0$, we have:

$$\begin{aligned} \lim_{r_i^{*} \to 0}(r_i^{*2} \times \ln r_i^{*}) &= \lim_{r_i^{*} \to 0}\left(\frac{\ln r_i^{*}}{r_i^{*-2}}\right) \\ &= \lim_{r_i^{*} \to 0}\left(\frac{\frac{1}{r_i^{*}}}{-2r_i^{*-3}}\right) \\ &= \lim_{r_i^{*} \to 0}\left(\frac{1}{r_i^{*-4}}\right) \\ &= 0 \end{aligned} \tag{3.6}$$

Thus, from equation (3.5) and by using equation (3.6), the equation (3.7) can be obtained:

$$\lim_{r_i^{*} \to 0} W = 2\pi \tag{3.7}$$

This shows W is always a constant number in the cylinder ($r_i^* \approx 0$).

Fig 3.1a illustrates this character very clearly. The constant number is 2π.

2) The velocity of W with the changing of r_i^*

Take the limit of the reciprocal of w with $r_i^* \to 1$, it shows:

$$\lim_{r_i^* \to 1} \frac{1}{W} = \lim_{r_i^* \to 1} \left(\frac{r_i^{*2} \times \ln r_i^* + \frac{1}{2}(1 - r_i^{*2})}{\pi(1 - r_i^{*2})} \right)$$

$$= \lim_{r_i^* \to 1} \frac{\ln r_i^*}{-\pi}$$

$$= 0 \tag{3.8}$$

Base on the equation (3.5), we can explain this phenomena from a mathematical point of view.

The velocity of the term $(r_i^{*2} \ln r_i^*) \to 0$ in the denominator of the equation (3.5) is faster than the term $(1 - r_i^{*2}) \to 0$ in the numerator of the equation (3.5). This makes $W \to \infty$, when $r_i^* \to 1$.

The physical meaning is that when the distance D between two concentric cylinders is very small, the heat flux Q released or absorbed in the melting/freezing process is also very small. However, in this situation, the time required for $R^* = r_i^*$ in

the melting/freezing process is smaller than the Q. These results produced in the heat transfer per unit time are much bigger.

Referring to Fig 3.1b, we can see when $r_i^* > 0.9$ approximately, W increases dramatically when the distance D between two concentric cylinders decreases. However, when $r_i^* < 0.9$, the W increases very slowly when the distance D between two concentric cylinders decreases.

For the freezing process, the same results will be obtained as for the melting process.

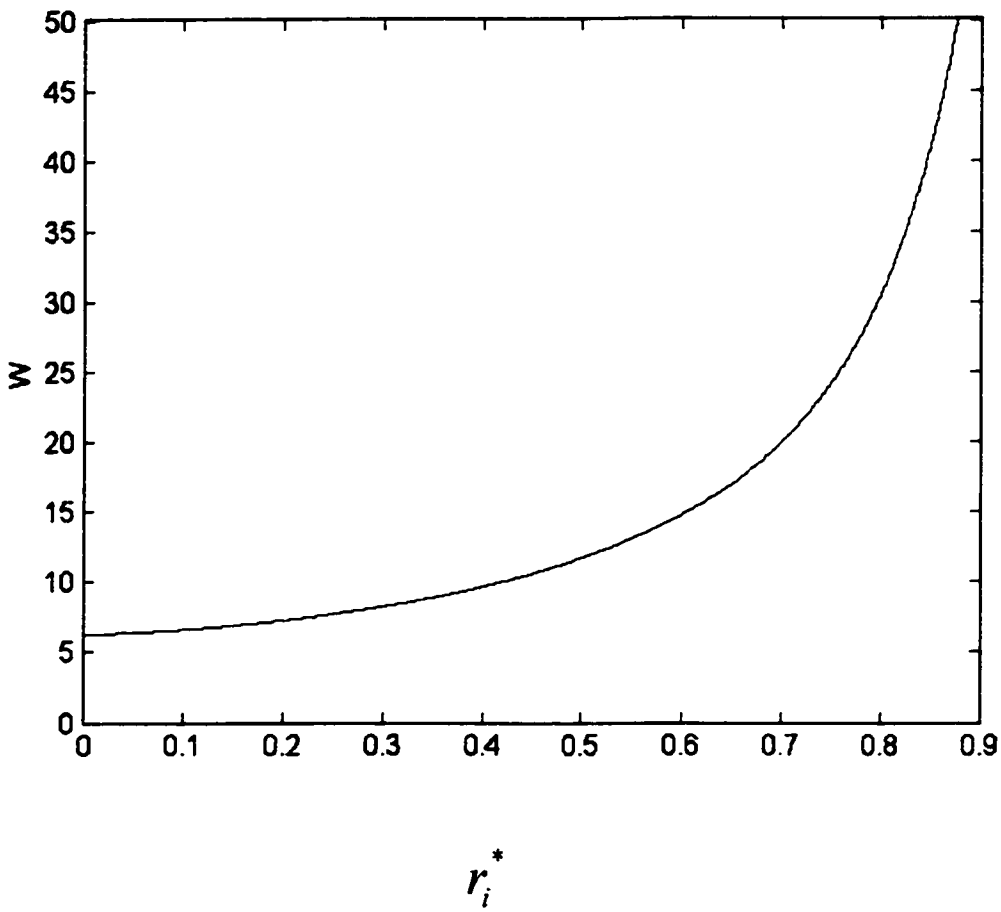

Fig 3.1a Schematic diagram of the relationship between W and r_i^*

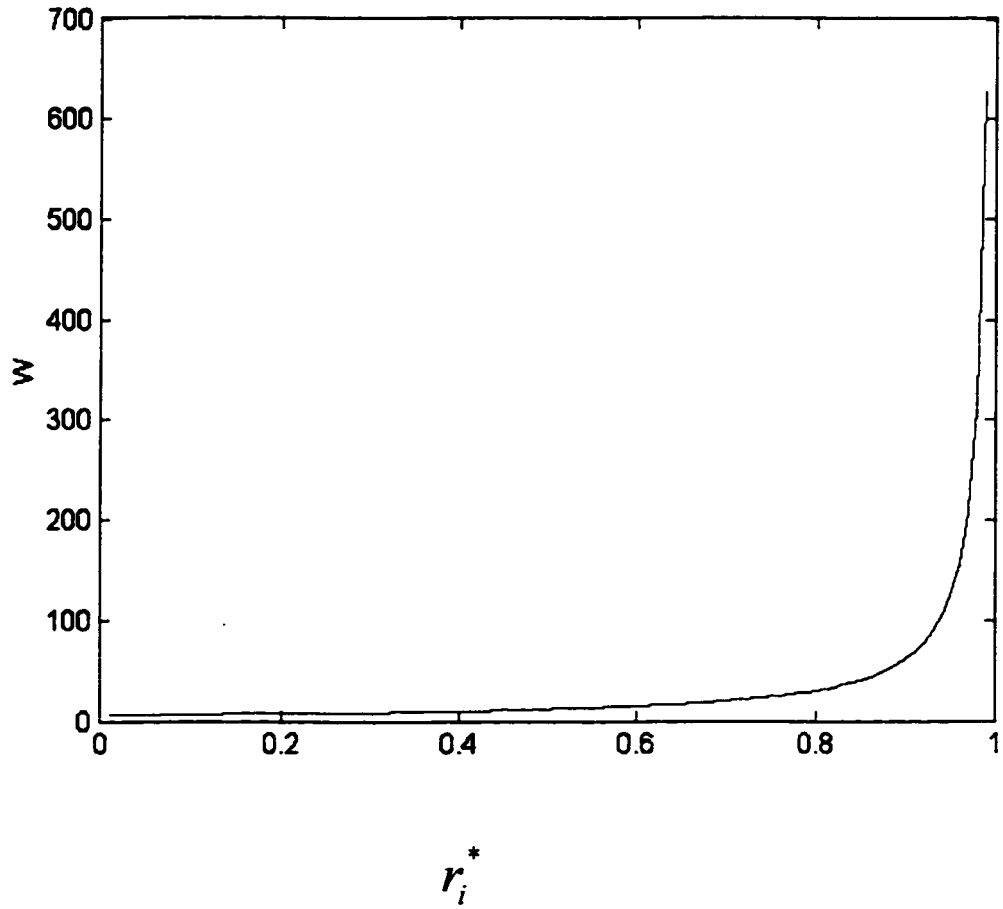

Fig 3.1b Schematic diagram of the relationship between W and r_i^*

3.2 The Extreme Value Analysis of the Phase Front Velocity

The phase front velocity, presented in equation (2.79) or (2.83), is presented in this section. Figure 3.2 show that the phase front velocity has a maximum value. The location of the maximum value can be determined by differentiating equation (2.79) or (2.83) with respect to R* and then equating the result to zero.

$$R^{*} = \frac{1}{e}$$

$$= 0.3679 \tag{3.9}$$

Substitution of equation (3.9) into equation (2.79) gives:

$$\left(\frac{dR^{*}}{dt^{*}}\right)_{\max} = -2.718 S_T \tag{3.10}$$

This means maximum value of $\left(\frac{dR^{*}}{dt^{*}}\right)$ exists at the location $R^{*} = 0.3679$.

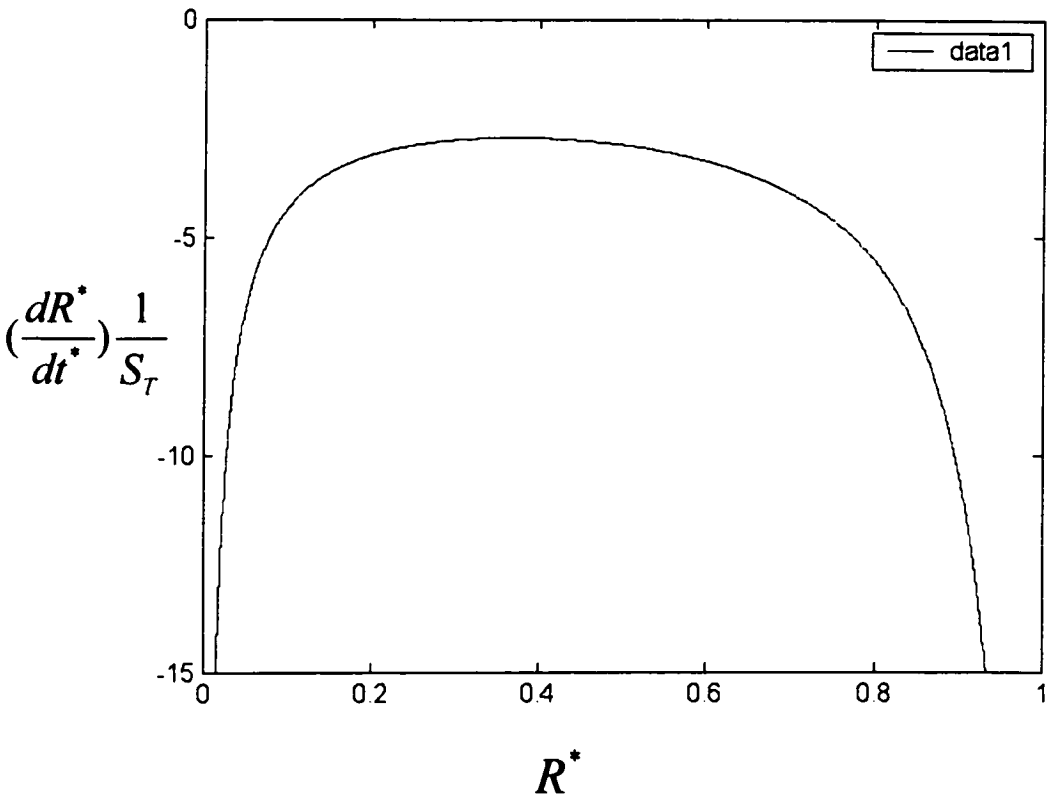

Fig.3.2 The relationship of $\frac{dR^*}{dt^*} * \frac{1}{S_T}$ with R^*

3.3 Theoretical Results Shown in the Diagram in the MFRD

In this section, the angle θ is also considered to be equal to π.

Figure 3.3a shows the melting and freezing fronts in the MFRD with the inner radius of $r_i^* = 0.3679$. This Figure is based on the calculation from equations (2.80), (2.84) and utilizing equations (2.63a), (2.63b) with the angle α rotating counter clockwise. Figure 3.3b shows the MFRD corresponding to Figure 3.3a.

The next consideration is the MFRD with the inner radius $r_i^* = 0$ as shown in Figure 3.4a. This Figure is calculated from equations (2.80), (2.84), (2.63a) and (2.63b) with the angle α rotating clockwise. Figure 3.4b shows the MFRD corresponding to Figure 4.5a.

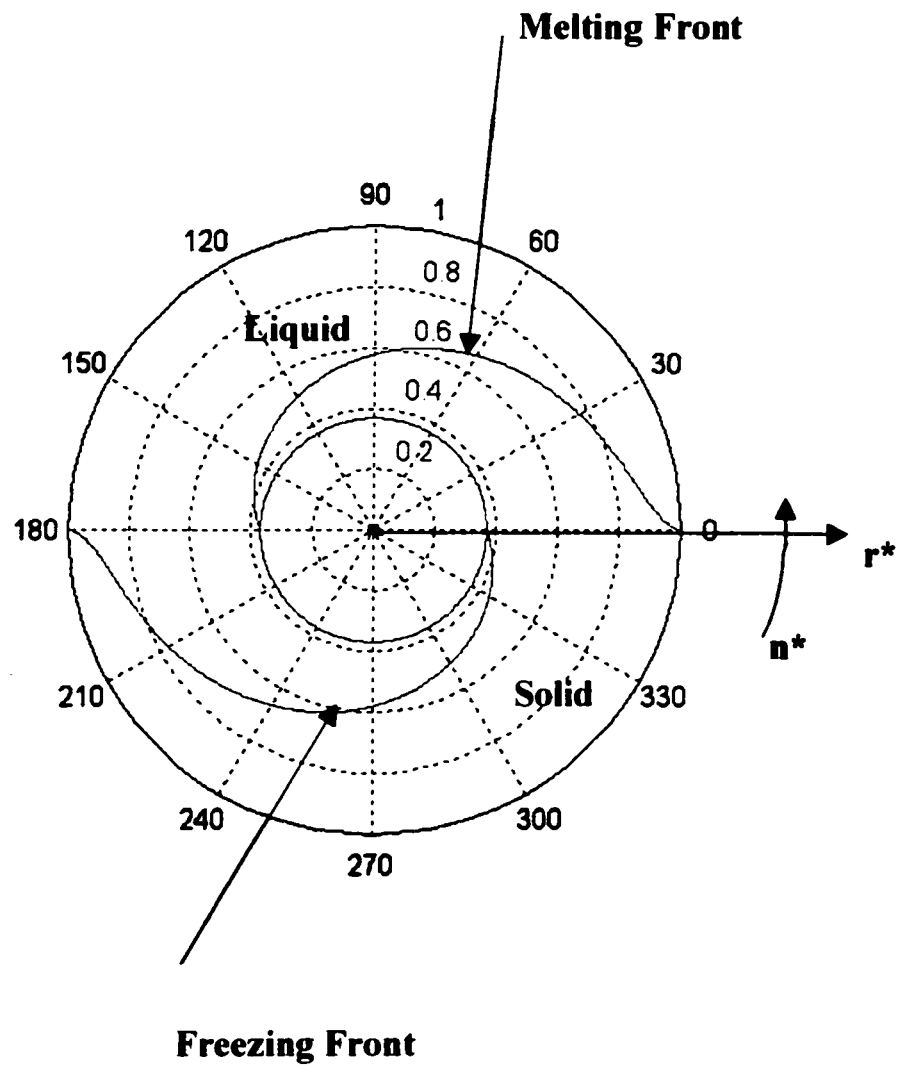

Fig. 3.3a Schematic diagram of melting-freezing fronts with the inner radius of 0.3679

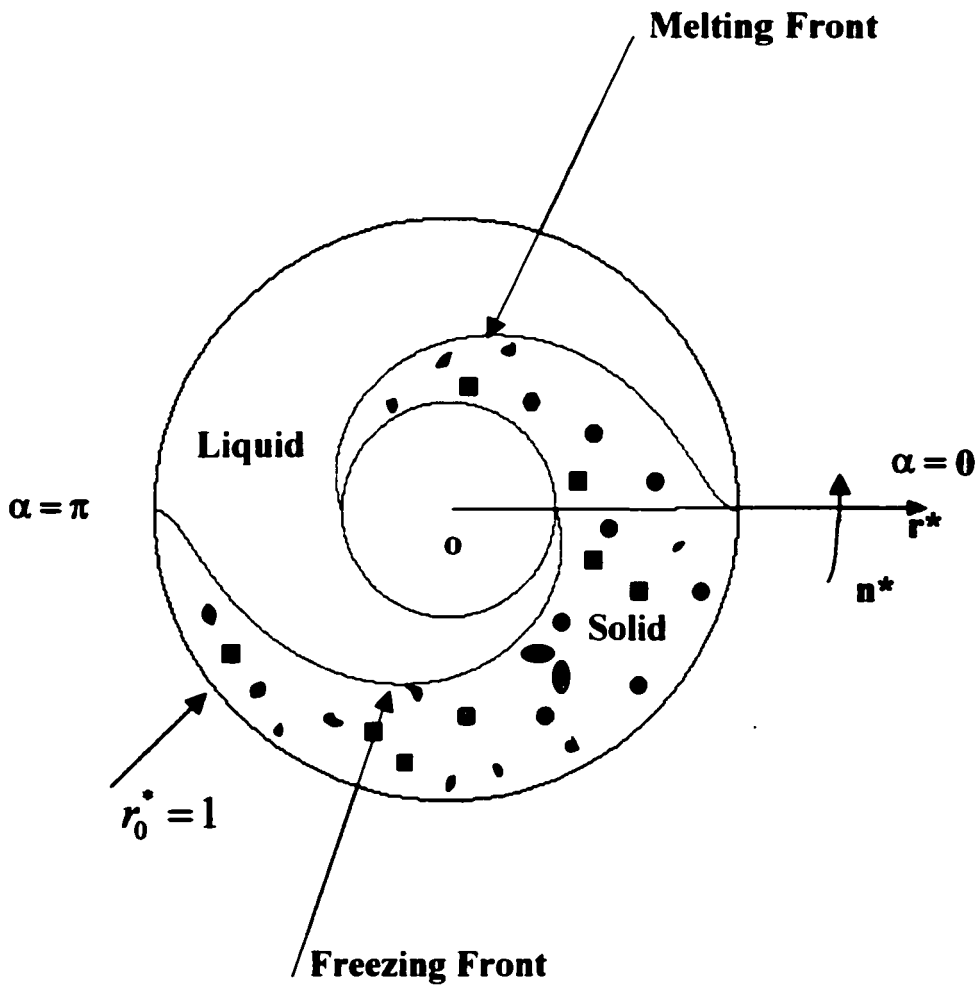

Fig. 3.3b The MFRD with the inner radius of 0.3679

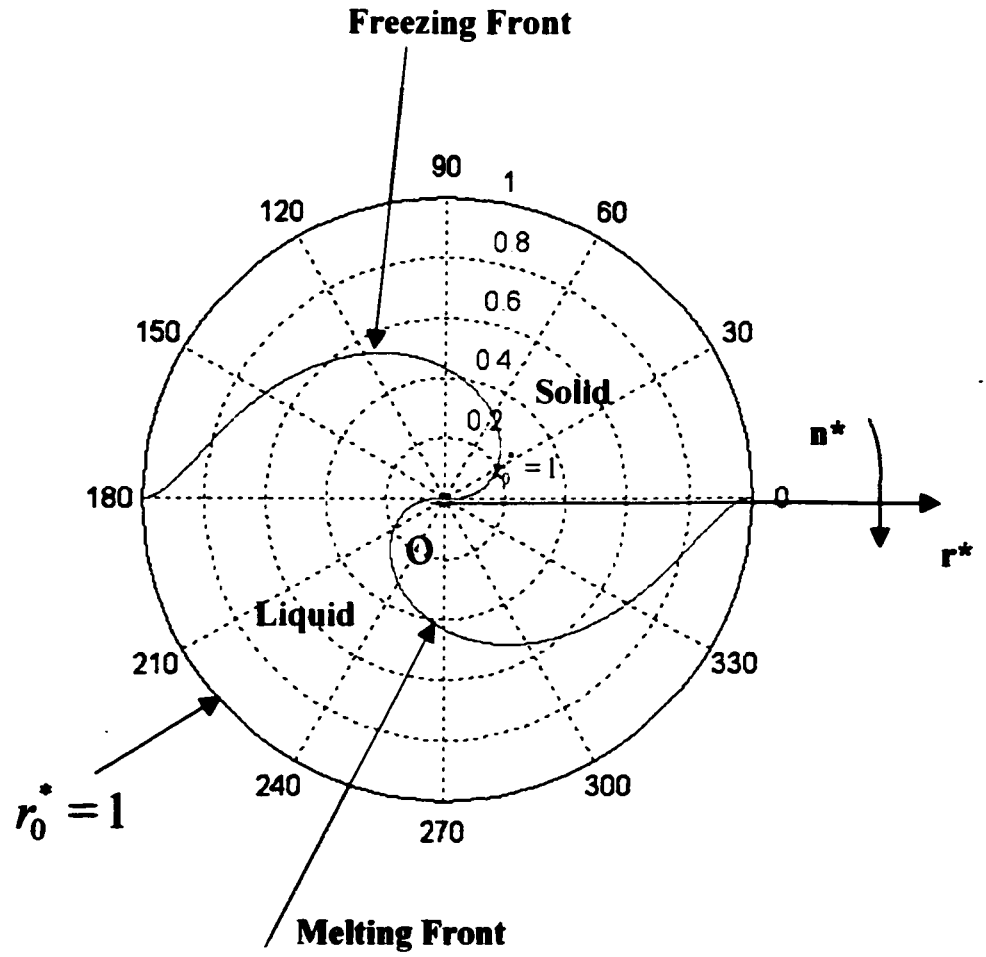

Fig 3.4a Schematic diagram of melting-freezing fronts with the inner radius of zero

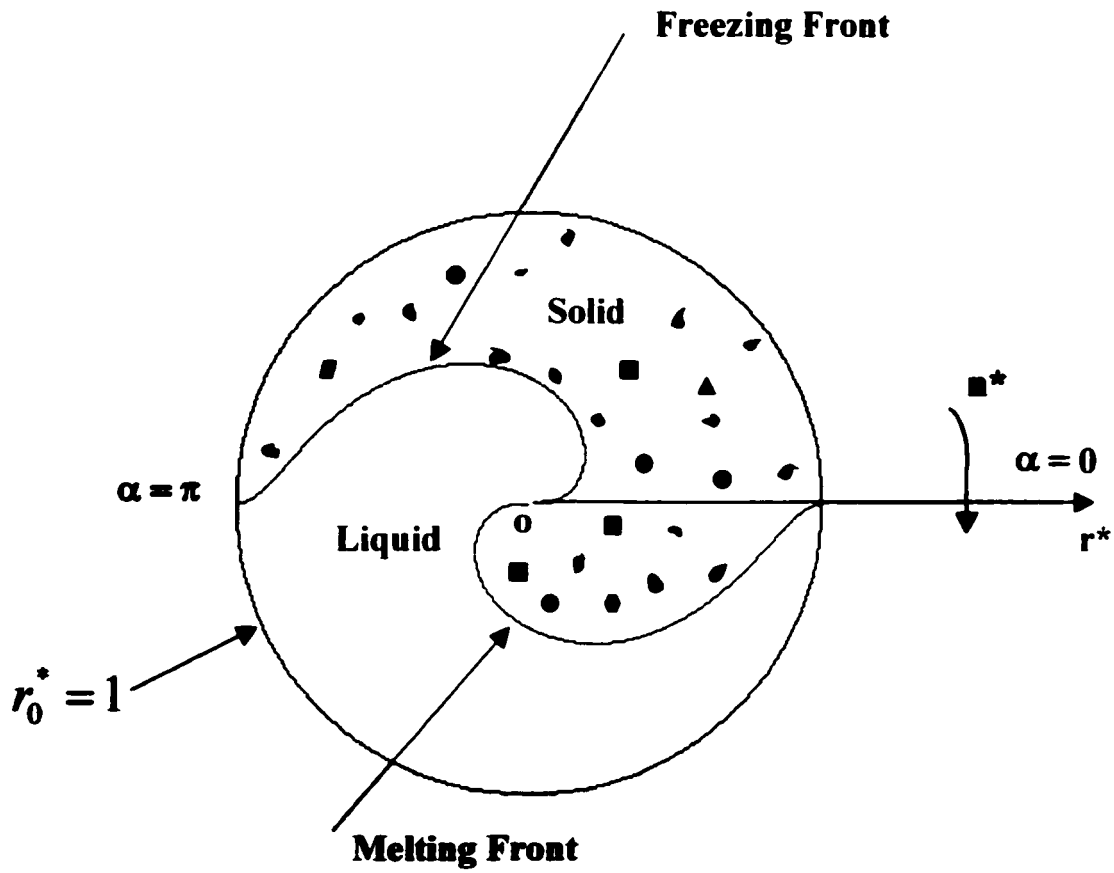

Fig 3.4b The MFRD of melting-freezing fronts with the inner radius of zer0

3.4 Numerical Results Shown in the Diagram in the MFRD

The numerical solution is calculated from the differential equations (2.76), (2.65) to (2.69) and for equations (2.77), (2.71) to (2.75) with finite differences.

Figure 3.5 shows the melting and freezing fronts in the MFRD with the inner radius of $r_i^* = 0.3679$. The finite difference thermal network model consists of sixteen hundred nodes along the tangential direction and nine nodes along the axial direction in the melting/freezing phase. The Figure is based on the numerical solution from the discretizing equations with the α angle- rotating counter clockwise

Figure 3.6 shows the melting and freezing fronts in the MFRD with the inner radius of $r_i^* = 0$. The finite difference thermal network model consists of twenty nine hundred nodes along the tangential direction and nine nodes along the axial direction in the melting/freezing phase. The Figure is based on the numerical solution from the discretizing equations with the angle α rotating clockwise.

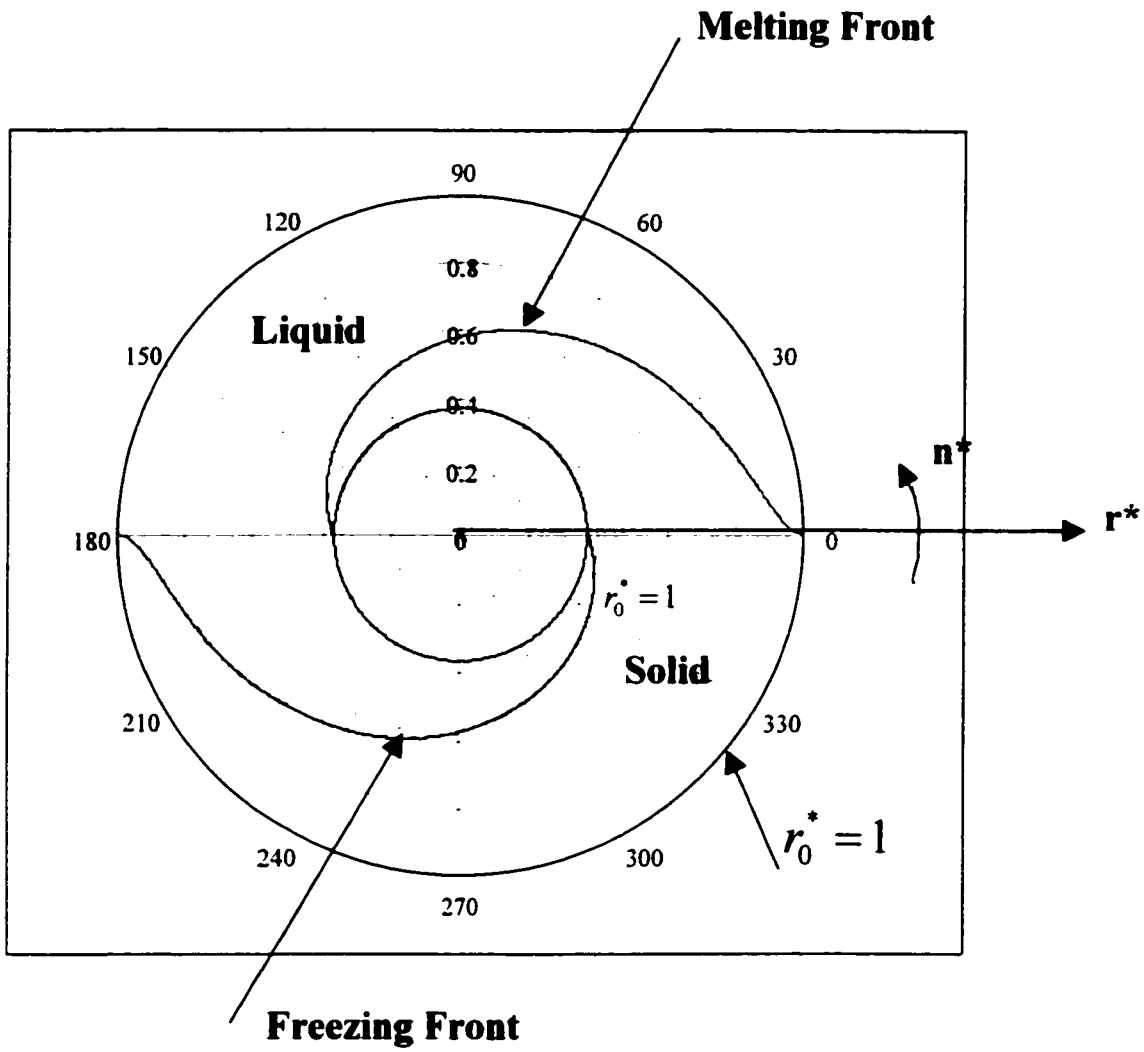

Fig 3.5 Schematic diagram of melting-freezing fronts with the inner radius of 0.3679

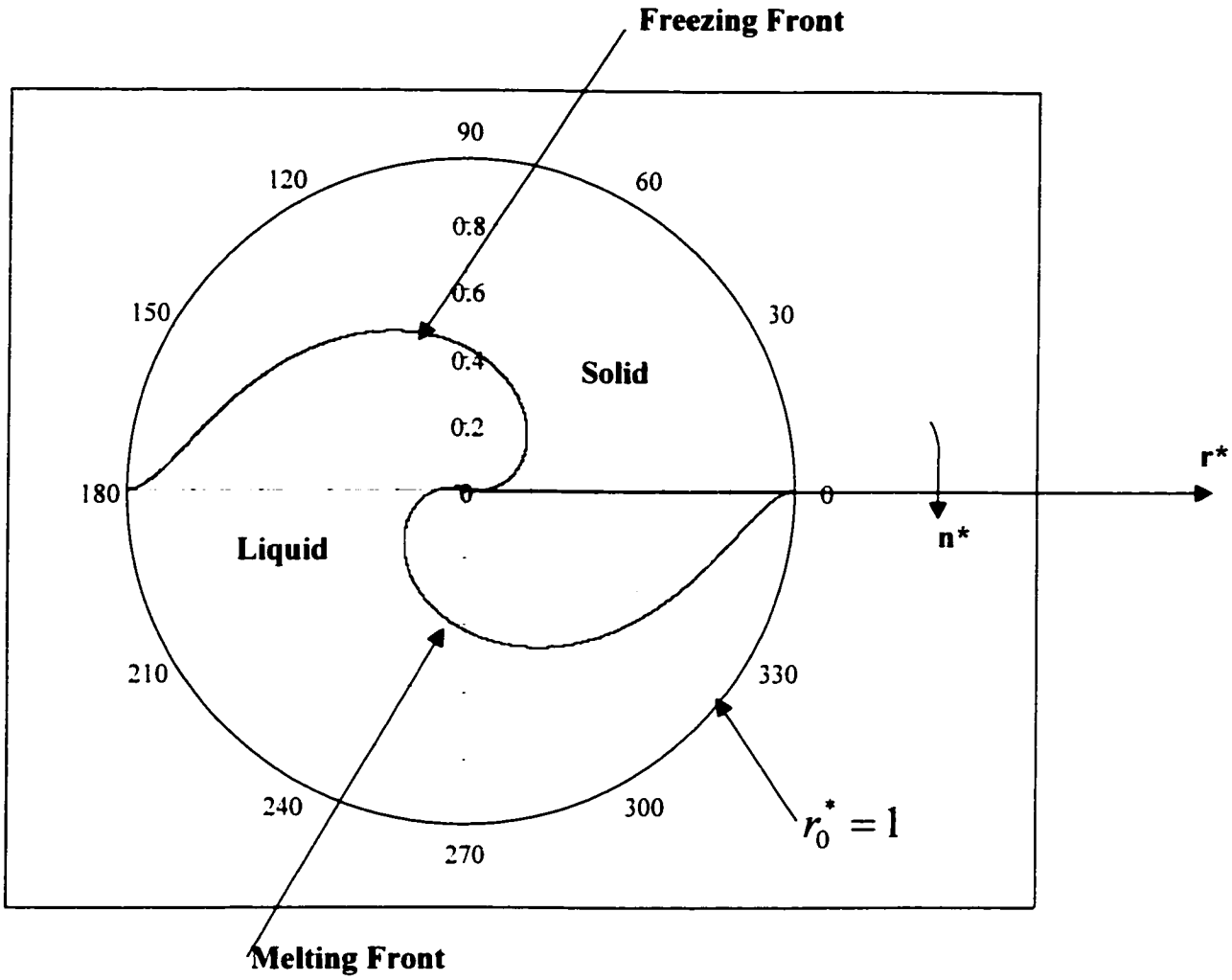

Fig 3.6 Schematic diagram of melting-freezing fronts with the inner radius of zero

CHAPTER 4

Discussion

4.1 The Example of Application

The most important character of the use of PCMs is the thermal storage process occurring at a nearly constant temperature, which is typically desirable in aerospace. Therefore, the MFRD can be used as a new thermal design technique in the satellites, specifically, in a small spinning satellite.

Now in the aerospace technology, the methods of thermal design in the thermal control subsystem are as follows:

1) OSR (Optical Solar Reflector, which is low absorptivity and high emissivity ε)
2) MLI (Multi-Layers Insulation Materials, which is low absorptivity and low emissivity ε)
3) Coating
4) Heat pipes
5) Thermal dissipate panels
6) Cu-KCu (copper-constantan) heating sheets

PCMs have been little used as the thermal design in aerospace. From the previous study, MFRD can replace OSR and the coating, which are used in the outer panels of satellites, because for the small capacity satellite, the decline of α of the coating or the OSR will make the thermal design more complicated. For example, at the end of the life of the small satellite, the solar absorptivity α in the outer panels increases. This also results in an increase of the solar heating of small satellites. The surface of area is not great enough to release the heat flux into outer space. The use of the MFRD can solve this problem very well by using a large latent of solidification of the PCM. Furthermore, the device can maintain the temperature of modules in the satellites at or near the solidification temperature of the PCM in the MFRD.

Of course, there is still a lot of work to be done in the application of MFRD for spacecraft. For example, the thermal vacuum, thermal equilibrium experiments and environmental, ambient noise experiments, vibration experiment should be performed with the MFRD.

CHAPTER 5

Summary

5.1 Summary

Based on the exact solutions, the design parameters, θ, D, n and D/r_o are determined. The most important design parameter is the dimensionless geometric ratio, D/r_o in industrial use. In order to determine the geometric dimensions of D and r_o individually from the ratio of D/r_o, the radius of the outer cylinder, r_o, should be set first. Then the value of D can be determined from the ratio D/r_o. After the determination of D and r_o, the rotating speed of the device, n, can be obtained from equation (2.50).

After the MFRD is built, the ratio D/r_o cannot be changed anymore. However, with a fixed geometric ratio, D/r_o, the rotating speed of the device, n, can be regulated, by using equation (2.50), to reach the designed performance when the amount of the heat to be transferred from the heat source varies. Therefore, the MFRD has a good capability of maintaining the design condition, when the amount of heat transferred from the heat source changes.

From the above discussion, the MFRD can be used as a heat exchanger to transfer continuously heat from a heat source to a heat sink. Especially, it can be used in the spinning small satellite to solve some thermal design difficulties. Thus, its future use in aerospace is good.

CHAPTER 6

Future Work

6.1 Recommendations of Future Work

The intended Future work is given in the following directions:

1. Numerical simulation of the melting and freezing processes taking place in the MFRD, formulated by the system of equations (2.6b) to (2.17).
2. Theoretical and numerical analysis with the temperature variation of the heat source and the heat sink in the direction along the rotating angle α.
3. Considering the boundary surface of the heat source/heat sink subjected to heat fluxes and to radiation into ambient.
4. Investigating the stability of the thermal proprieties of PCMs in MFRD in some rigorous condition after a few years.
5. Analyzing the one dimensional or multidimensional phase-change problems with natural convection present at the interface.

REFERENCES

1 Sui Lin and Tzu-Fang Chen, "Design Analysis On Melting-Freezing Rotating Device Transferring Heat From A Heat Source To A Heat Sink". J. of Thermal Science.

2. Mills, A.F., "Heat Transfer", Richard D. Irwin, Boston, Chap. 7, 1982.

3. Rabin, Y. and Korin, E., "Incorporation of Phase-Change Materials Into a Ground Thermal Energy Storage System: Theoretical Study", Transactions of the ASME, Journal of Energy Resources Technology, Vol. 118 , No. 3 , 1996, pp. 237-241.

4. Esen, M. and Ayhan, T., "Development of a model compatible with solar assisted cylindrical energy storage tank and variation of stored energy with time for different phase change materials", Energy Conversion and Management, Vol. 37 , No. 12 , 1996, pp. 1775-1786.

5. Adebiyi, G. A., Hodge, B. K. and Steele, W. G., Jalalzadeh-Azar, A. and Nsofor, E. C., "Computer Simulation of a High-Temperature Thermal Energy Storage System Employing Multiple Families of Phase-Change Storage Materials", Transactions of the ASME, Journal of Energy Resources Technology, Vol. 118 , No. 2 , pp. 1996,102-111.

6. Lu, D. M., Simpson, H., C. and Gilchrist, A., "Conjugate Heat Transfer Analysis of Fluid Flow in a Phase-Change Energy Storage Unit", International Journal of Numerical Methods for Heat and Fluid Flow, Vol. 6 , No. 3 , 1996, pp. 77-90.

7. Jalalzadeh-Azar, A. A., Steele, W. G. and Adebiyi, G. A., "Heat Transfer in a High-Temperature Packed Bed Thermal Energy Storage System -- Roles of Radiation and Intraparticle Conduction", Transactions of the ASME, Journal of Energy Resources Technology, Vol. 118 , No. 1 , 1996, pp. 50-57.

8. Zhang, Y. and Faghri, A., "Heat transfer enhancement in latent heat thermal energy storage system by using the internally finned tube", International Journal of Heat and Mass Transfer,Vol. 39 , No. 15 , 1996, pp. 3165-3174.

9. El-Dessouky, H. and Al-Juwayhel, F., "Effectiveness of a thermal energy storage system using phase-change materials", Energy Conversion and Management, Vol. 38 , n. 6 , 1997, pp. 601-618.

10. Gong, Z-X. and Mujumdar, A. S., "Thermodynamic optimization of the thermal process in energy storage using multiple phase change materials", Applied Thermal Engineering, Vol. 17 ,No. 11, 1997, pp. 1067-1084.

11. Kurklu, A., "Energy storage applications in greenhouses by means of phase change materials (PCMs): A review", Renewable Energy, Vol. 13 , No. 1 , 1998, pp. 89-104.

12. Aceves, S. M., Nakamura, H., Reistad, G. M. and Martinez-Frias, J., "Optimization of a Class of Latent Thermal Energy Storage Systems With Multiple Phase-Change Materials", Transactions of the ASME, Journal of Solar Energy Engineering, Vol. 120 , No. 1, 1998, pp. 14-19.

13. Lacroix, M. and Duong, T., "Experimental improvements of heat transfer in a latent heat thermal energy storage unit with embedded heat sources", Energy Conversion and

Management, Vol. 39 , No. 8 , 1998, pp. 703-716.

14. Costa, M.., Buddhi, D. and Oliva, A., "Numerical simulation of a latent heat thermal energy storage system with enhanced heat conduction", Energy Conversion and Management, Vol 39, 1998, pp. 319-330.

15. Glakpe, E. K., Cannon, J. N. and Kerslake, T. W., "Modeling cyclic phase change and energy storage in solar heat receivers", J. Thermophysics and Heat Transfer, Vol 12, 1998, pp. 406-41.

16. Yimer, B. and Senthil, K., "Experimental and analytical phase change heat transfer", Energy Conversion and Management, Vol 39, 1998, pp.889-897.

17. El-Dessouky, H. T., Bouhamra, W. S., Ettouney, H. M. and Akbar, M., "Heat Transfer in Vertically Aligned Phase Change Energy Storage Systems", Transactions of the ASME, Journal of Solar Energy Engineering, Vol. 121, No. 2, 1999, pp. 98-109.

18. Muntasser, M. A., Dibirov, M. A., Kenisarin, M. M. and Mozgovoy, A. G., "Direct Conversion of Solar Energy into Electric-Energy - Inorganic Salt Crystallohydrates as Phase-Change Materials for Low-Grade Solar Energy Storage", Applied Solar Energy, Vol. 36, No. 3, 2000, pp. 57-66.

19. Wang, X., Lu, E., Lin, W. and Wang, C., "Micromechanism of heat storage in a binary system of two kinds of polyalcohols as a solid-solid phase change material", Energy Conversion and Management, Vol. 41, No. 2, 2000, pp. 135-144.

20. Sokolov, P., Ibrahim, M. and Kerslake, T., "Computational Heat-Transfer Modeling of

Thermal Energy Storage Canisters for Space Applications". Journal of Spacecraft and Rockets, Vol. 37, No. 2, 2000, pp. 265-272.

21. George A. Lane, "Solar Heat Storage Latent heat Material Volume I". CRC Press, Inc. Boca Raton, Florida, Chap. II, 1980.

22. Bejan, A., "Heat Transfer", John Wiley & Sons, New York, Chap.3, 1993.

23. Carslaw, H. S. and Jaeger, J.C., "Conduction of Heat in Solids", Oxford University Press, London, Chap.11, 1959